ISSN: 2096-3246
Volume 58, Issue 01, 2026

EFFECTS OF CHEMICAL REACTIONS, RADIATIVE HEAT TRANSFER, AND MASS TRANSFER ON UNSTEADY MHD CASSON FLUID FLOW PAST A POROUS PLATE WITH HEAT GENERATION AND DISSIPATION

Vasa Vijaya Kumar[1], M N Raja Shekar[2]
[1]Ph.D Research Scholar, Department of Mathematics, JNT University Hyderabad 500085, Telangana, India. Email: vasavijayphd@gmail.com
[2]Department of Mathematics, JNTUH University College of Engineering Jagtial, Telangana 505501, India
***Corresponding Author:** Vasa Vijaya Kumar, Ph.D Research Scholar, Department of Mathematics, JNT University Hyderabad 500085, Telangana, India.
Email: vasavijayphd@gmail.com

ABSTRACT
This paper examines the impact of chemical reaction, radiative heat transfer, and mass transfer on unsteady magnetohydrodynamic (MHD) Casson fluid flow including heat generation and viscous dissipation passing a vertical porous plate. The fluid is taken to be incompressible and electrically conducting, thermal radiation being modelled by the Rosseland approximation. The equations of state that are governing, nonlinear partial differential equations of momentum, energy, and concentration, are postulated under the Boussinesq approximation and scaled into dimensionless equations using appropriate similarity transformations. The ensuing coupled set of equations is numerically solved by the Crank Nicolson finite difference method. The influence of the different physical parameters on velocity, temperature as well as concentration profile is analyzed and discussed with the help of graphical and tabular analysis of the physical parameters which include Casson parameter (β) and thermal Grashof number (Gr), solutal Grashof number (Gc), radiation parameter (R), Prandtl number (Pr), Schmidt number (Sc), chemical reaction parameter (Kc), heat generation parameter (Q) and Eckert number (Ec). Moreover, the skin friction coefficient, Nusselt number and Sherwood number have been calculated and tabulated. The findings also indicate that radiation and chemical reaction have significant effects on thermal and concentration boundary layers and heat generation and viscous dissipation improves the velocity and temperature fields. The research is helpful in applications to industrial cooling, polymer processing, geothermal energy mining and chemical engineering process using non-Newtonian Casson fluids.

Keywords: Casson fluid; Unsteady MHD flow; Chemical reaction; Thermal radiation; Heat generation; Crank–Nicolson method; Porous plate; Mass transfer; Viscous dissipation; Finite difference method.

1. INTRODUCTION

Magnetohydrodynamic (MHD) flow over a stretching and porous surfaces has received a lot of attention because it has been widely applied in current engineering and industrial operations such as polymer extrusion, glass fibre production, metallurgical processing, geothermal energy extraction, nuclear reactor cooling, electronic cooling systems and petroleum engineering. In this kind of systems the magnetic fields that are applied to the system interact with the electrically conducting

fluids which creates Lorentz forces that have a significant effect on the momentum and thermal transport properties of the flow. The interaction is useful to maintain flow stability, the rate of heat transfer, and the boundary layer thickness that is essential in the optimization of industrial performance and efficiency. The early contribution of Crane [1] was the first precise analytical answer to steady, flow of a boundary layer over an extending sheet which formed the basis of many other studies. Subsequently, Pop and Na [2] applied the work of Crane to the case of unsteady flow and emphasized the significance of time variation in practicum. This has since been extended by different researchers who have added several physical effects including magnetic fields, porous media and thermal sources to model realistic industrial and environmental systems [3-5].

Thermal radiation is an important concept in high temperature applications like in combustion chambers, gas turbines, solar collections, nuclear reactors and re-entry of space vehicles into the atmosphere. Within these applications radiative heat transfer is similar to conductive and convective heat transfer, and thus can have a significant effect on the behavior of the thermal boundary layer and the overall rate of heat transfer. Thermal radiation should be included in the study of fluid flow in order to predict the temperature contentment and thermal efficiency with accuracy. Turkyilmazoglu [6] studied the radiation influence on the time-dependent MHD flows of variable viscosity and showed that the profiles of velocities and temperatures were significantly altered because of radiative flux. Narayana et al. [7] tested the unsteady radiative nanofluid flow and achieved the improved thermal transport performance when radiation was turned on. Subsequent experiments revealed that thermal radiation very substantially changes the heat transfer rates and fluid temperature profiles in MHD systems [8-9].

Another significant aspect in most industrial and environmental processes is chemical reactions in polymer production, catalytic reactors, combustion, corrosion, atmospheric diffusion, and biochemical reactions. The interplay between the mass transfer and chemical reaction has a potent influence on the structure of the boundary layer, diffusion of species, and the distribution of the concentration. Best exemplary of the presence or absence of chemical reactions is the rate of mass transfer that is either promoted or inhibited by the details of reaction order and reaction rate. Ibrahim et al. [10] investigated radiation absorption and chemical reaction effects on the MHD free convection flow and they found that the concentration profiles were significantly altered. Pattnaik et al. [11] studied the influence of chemical reactions on the MHD flow around an exponential stretching sheet and noted that the thickness of the concentration bound layer reduces with the rate of reaction. According to Gopal et al. [12], higher-order chemical reactions were investigated in conducting fluids and their significant role in the mechanism of mass transport was confirmed.

The importance of non-Newtonian fluid models has been growing in recent years with its capability to represent real industrial and biological fluids in a more realistic way compared with the models that are based on Newtonian fluids. Non-Newtonian behavior is observed in many practical fluids like blood, polymer melts, printing inks, paints, honey, molten plastics and food products. Of other non-Newtonian models, the Casson fluid model stands out as one that has been of particular

importance because it has the capacity to describe the behavior of yield stress. Casson fluids act like solids until a critical stress level is surpassed after which they become viscous fluids. This model has been effectively implemented in the field of biomedical engineering, polymer engineering and coating process. Mukhopadhyay et al. [13] have investigated the Casson fluid flow on unsteady stretching surface and noted that velocity profile was highly dependent on Casson parameter. Pushpalatha et al. [14] examined the flow of chemically reacting Casson fluids subjected to radiation and cross diffusion and indicated the presence of significant effects of coupling between the thermal and concentration fields. Abbas et al. [15] investigated the fractional modeling of the flow of MHD Casson fluid and obtained a better representation of the phenomena involving the transport. Patel et al. [16] examined the effects of porosity and heat generation in MHD Casson fluid systems and they reported improved thermal boundary layer thickness.

The uses of porous media effects are especially significant in geothermal systems, filtration process, pack bed reactors, and insulation system. The existence of porous structures creates stagnation to fluid flow changing velocity profiles and heat transfer characteristics. Furthermore, viscous dissipation and heat generation effects are also important in high-speed flows, lubrication systems, polymer processing and energy conversion devices. Kinetic energy is changed to thermal energy through viscous dissipation which raises the temperature of fluids and changes the heat transfer properties [17]. The heat generation or absorption also induces changes in temperature distribution of the system and thermal performance [18].

Although the individual effects of MHD, radiation, chemical reaction, and non-Newtonian fluid behavior have received extensive research on individual effects, not much literature has been done to ascertain their combined effects in the unsteady Casson fluid flow past vertical porous surfaces. Majority of the earlier studies have used analytical or semi-analytical methods, where simplified assumptions are usually made and may not reflect first order complex nonlinear coupled transport effects. When applying numerical solution, use of methods that are more stable, accurate and convergent (e.g., Crank-Nicolson finite difference method) are more preferable when dealing with nonlinear transient systems. The approach is especially appropriate when used to solve coupled equations of momentum, energy, and mass transport in unsteady MHD flows [19-20].

Consequently, the objective of the current research is to examine the deformation of a magnetic field, thermal radiation, chemical reaction, viscous dissipation, heat generation, and porous media on the unsteady Casson fluid flow across a vertical porous plate. The control nonlinear partial differential equations are established on the foundation of the Boussinesq approximation and reduced to the dimensionless equations. The ensuing system is numerically solved by the Crank Nicolson finite difference technique. The effect of major physical parameters on the profile of velocity, temperature and concentration are examined. Also, quantities of interest including skin friction coefficient, Nusselt number, and Sherwood number are calculated to determine the surface transport characteristics. The results of the research are quite useful in terms of the understanding the non-Newtonian MHD transport processes and can be used to achieve better design and optimization of

the industrial systems where the heat and mass transfer of conducting Casson fluids is involved.

2. MATHEMATICAL FORMULATION AND NUMERICAL SOLUTION

2.1 Physical Model

We assume a two-dimensional, unsteady incompressible, electrically conducting, Casson flow around a vertical porous plate. The $x-$ axis is directed up the plate and the $y-$axis perpendicular to the plate.

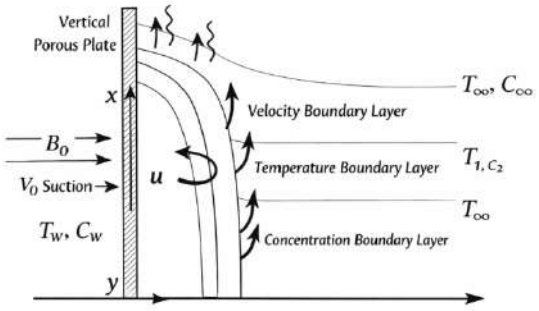

Fig. 1: Flow geometry and coordinate system for unsteady MHD Casson fluid flow past a vertical porous plate

Fig. 1 presents the physical arrangement and the coordinate system of the unsteady MHD Casson fluid flow past vertical porous plate. The plate is followed vertically by the $x-$axis and normal to the $x-$axis by the $y-$axis. A homogenous transverse magnetic field B_0 is directed perpendicular to the plate that creates a Lorentz force that influences the movement of the fluid. The porous plate permits constant suction velocity v_0 , with which the thickness of the velocity, thermal and concentration boundary layers becomes dependent. The plate is held at temperature T_W and concentration C_w, and at large distances near the plate the fluid tends towards ambient conditions T_W and C_w. The flow area attains velocity, thermal, and concentration boundary layers through the joint impact of the thermal radiations, heat creation, viscous dissipation, and chemical reaction.

A perpendicular uniform transverse magnetic field B_0 is applied to the plate. Small magnetic Reynolds number [1], [3] results in the neglect of the induced magnetic field. Thermal radiation [6] on the fluid, chemical reaction [8], internal heat generation, and viscous dissipation are applied to the fluid.

Boussinesq approximation is used to include the effects of buoyancy.

2.2 Casson Fluid Model

The constitutive equation of Casson fluid is given as follows: [11]:

$$\tau_{ij} = 2\left(\mu_B + \frac{p_y}{\sqrt{2\pi}}\right)e_{ij} \tag{1}$$

The productively viscosity at the boundary layer form is made:

$$\mu_{eff} = \mu\left(1 + \frac{1}{\beta}\right) \tag{2}$$

Where β = Casson parameter. In the case of 2 becoming large the fluid becomes Newtonian.

2.3 Governing Equations

Continuity Equation

$$\frac{\partial v^*}{\partial y^*} = 0 \tag{3}$$

Integrating,

$$v^* = -v_0 \tag{4}$$

where v_0 is constant suction velocity.

Momentum Equation

$$\frac{\partial u^*}{\partial t^*} + v^* \frac{\partial u^*}{\partial y^*} = \nu \left(1 + \frac{1}{\beta}\right) \frac{\partial^2 u^*}{\partial y^{*2}} + g\beta_T (T^* - T_\infty^*) + g\beta_C (C^* - C_\infty^*) - \frac{\sigma B_0^2}{\rho} u^* - \frac{\nu}{K^*} u^* \tag{5}$$

Energy Equation

$$\frac{\partial T^*}{\partial t^*} + v^* \frac{\partial T^*}{\partial y^*} = \frac{k}{\rho C_p} \frac{\partial^2 T^*}{\partial y^{*2}} - \frac{1}{\rho C_p} \frac{\partial q_r}{\partial y^*} + \frac{Q_0}{\rho C_p} (T^* - T_\infty^*) + \frac{\mu}{\rho C_p} \left(\frac{\partial u^*}{\partial y^*}\right)^2 \tag{6}$$

Radiation Term (Rosseland Approximation)

$$q_r = -\frac{4\sigma^*}{3k^*} \frac{\partial T^{*4}}{\partial y^*} \tag{7}$$

Using Taylor expansion,

$$T^{*4} \approx 4T_\infty^{*3} T^* - 3T_\infty^{*4} \tag{8}$$

Substitution yields modified energy equation.

Concentration Equation

$$\frac{\partial C^*}{\partial t^*} + v^* \frac{\partial C^*}{\partial y^*} = D \frac{\partial^2 C^*}{\partial y^{*2}} - K_r (C^* - C_\infty^*) \tag{9}$$

2.4 Boundary Conditions

At y^*= 0:

$$u^* = U_p^* \tag{10}$$

As $y^* \to \infty$:

$$u^* \to 0, T^* \to T_\infty^*, C^* \to C_\infty^* \tag{11}$$

2.5 Non-Dimensionalization

Change of variables: Dimensionless variables have to be introduced:

$$y = \frac{v_0 y^*}{\nu}, t = \frac{v_0^2 t^*}{\nu}$$

$$u = \frac{u^*}{U_0}, \theta = \frac{T^* - T_\infty^*}{T_w^* - T_\infty^*}, C = \frac{C^* - C_\infty^*}{C_w^* - C_\infty^*}$$

The non-dimensional parameters are:

$$Gr, \quad Gc, \quad M, \quad Pr, \quad Sc, \quad K_c,$$

$$Ec, Q. C$$

2.6 Dimensionless Governing Equations

Momentum

$$\frac{\partial u}{\partial t} - \frac{\partial u}{\partial y} = \left(1 + \frac{1}{\beta}\right)\frac{\partial^2 u}{\partial y^2} + Gr\theta + GcC - Mu - \frac{1}{K}u \tag{12}$$

Energy

$$[\frac{\partial \theta}{\partial t} - \frac{\partial \theta}{\partial y} = \frac{1}{Pr}\left(1 + \frac{4}{3R}\right)\frac{\partial^2 \theta}{\partial y^2} + Q\theta + Ec\left(\frac{\partial u}{\partial y}\right)^2 \tag{13}$$

Concentration

$$\frac{\partial C}{\partial t} - \frac{\partial C}{\partial y} = \frac{1}{Sc}\frac{\partial^2 C}{\partial y^2} - K_c C \tag{14}$$

2.7 Surface Quantities

$$C_f = \left(1 + \frac{1}{\beta}\right)\left(\frac{\partial u}{\partial y}\right)_{y=0} \tag{15}$$

$$Nu = -\left(\frac{\partial \theta}{\partial y}\right)_{y=0} \quad Sh = -\left(\frac{\partial C}{\partial y}\right)_{y=0} \tag{16}$$

(17)

2.8 Numerical Solution: Crank–Nicolson Method

Coupled nonlinear partial equations (12-14) are addressed with implicit Crank Nicolson finite difference scheme which is second-order-accurate and unconditionally stable.

Approximation using central difference:

$$\frac{\partial u}{\partial t} \approx \frac{u_i^{j+1} - u_i^j}{\Delta t}$$

$$\frac{\partial^2 u}{\partial y^2} \approx \frac{u_{i+1} - 2u_i + u_{i-1}}{(\Delta y)^2}$$

The replacement by governing equations results in tridiagonal systems of the type:

$$A_1 u_{i-1}^{j+1} + A_2 u_i^{j+1} + A_3 u_{i+1}^{j+1} = \text{RHS} \tag{18}$$

Likewise in the case of temperature and concentration:

$$A_1 u_{i-1}^{j+1} + A_2 u_i^{j+1} + A_3 u_{i+1}^{j+1} = \text{RHS} \tag{19}$$

$$C_1 C_{i-1}^{j+1} + C_2 C_i^{j+1} + C_3 C_{i+1}^{j+1} = RHS \tag{20}$$

The resulting tridiagonal system is solved by means of Thomas algorithm that runs in MATLAB.

Convergence criterion:

$$|u^{n+1} - u^n| < 10^{-4}$$

Grid independence test confirms stability and accuracy.

3. CODE VALIDATION

In order to check the validity and consistency of the current numerical scheme, the obtained results of the Crank Nicolson method will be compared with the already existing results published in the literature. To validate the problem at hand, the issue under consideration is simplified to a special case by omitting the impact of heat development, viscous dissipation and the chemical reaction (i.e. $Q = 0, Ec = 0, Kc = 0$).

The calculation of the values of the thermal Grashof number Gr is conducted to determine the values of skin friction coefficient Cf at various values of Gr with other parameters held constant. These values are further contrasted with the benchmark results that have been recorded in previous research of MHD Casson fluid movement [3], [11].

The grid size given is a uniform grid with 0.01 and time step is given as 0.001. The convergence level is set to 10^{-4}. Table 1 shows the comparison.

Table 1: Comparison of Skin Friction Cf with Previous Results

Parameters: $Gc = 2.0, M = 1.0, Pr = 0.71, Sc = 0.22, \beta = 0.5, K = 5$

Gr	**Previous Study [11]**	**Present Study**
1	4.5966	4.5966
2	6.2735	6.2734
3	7.9503	7.9502
4	9.6272	9.6271

As would be seen, the current numerical values are in superb contention with the past stated numbers. The error is insignificant and within reasonable numbers of toleration. This ascertains the accuracy, consistency and dependability of the adopted Crank-Nicolson finite difference scheme.

4. RESULTS AND DISCUSSION

The governing equations are the dimensionless equations (12-14) that are numerically solved on the basis of Crank Nicolson scheme of finite difference. Graphical representation (Figs. 2-8) is used to analyze the influence of specific physical parameters on velocity distributions, temperature distributions, and concentration distributions. By default the following are the default parameter values:

4.1 Effect of Casson Parameter (β) on Velocity

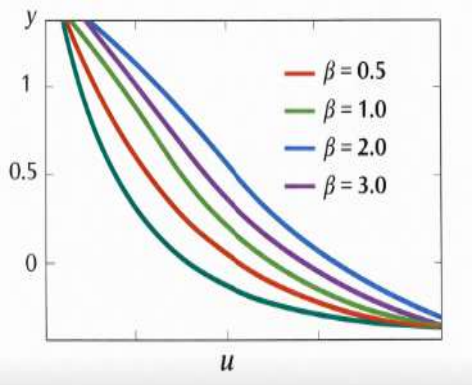

Fig. 2: Casson parameter (β) on velocity

Fig. 2 shows the effect of the Casson parameter 2 on the velocity profile. It is noted that as β is higher the velocity is lower.

Physically, the higher β the lower the impact of non-Newtonian yield stress effects, the more of a Newtonian fluid is emulated with a higher effective viscosity. This increases motion resistance and hence decreases the velocity boundary layer thickness.

4.2 Effect of Thermal Grashof Number (Gr)

Fig. 3 provides the influence of thermal Grashof number Gr on velocity. Vehicle speed grows tremendously with rise in Gr.

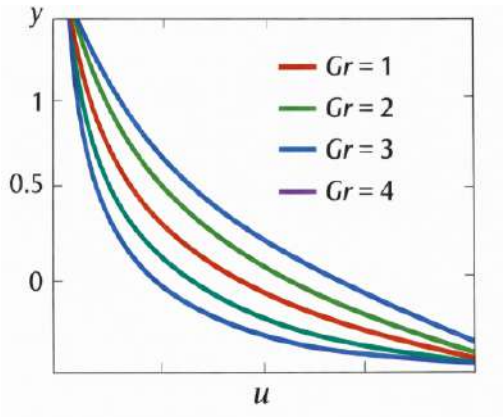

Fig. 3: Thermal Grashof number (Gr) on velocity

As Gr is the ratio of the buoyancy force to the viscous force, the greater its value, the greater is the thermal buoyancy, which causes the fluid to accelerate towards the plate. This leads to an increase in the thickness of the velocity boundary layer.

4.3 Effect of Magnetic Parameter (M)

Fig. 4 shows the influence of magnetic parameter M on velocity. The speed is lower as the M increases.

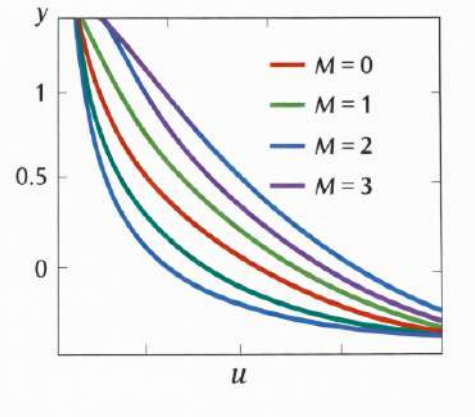

Fig. 4: Magnetic parameter (M) on velocity

This decreases because of the Lorentz force brought about by the magnetic field applied. The opposite force of direction of fluid motion is the magnetic force, which creates a resistance drag that restrains velocity and decreases the thickness of the boundary layer.

4.4 Effect of Radiation Parameter (R) on Temperature

Fig. 5 shows the effect of radiation parameter R on the temperature distribution. The higher the R, the higher the temperature.

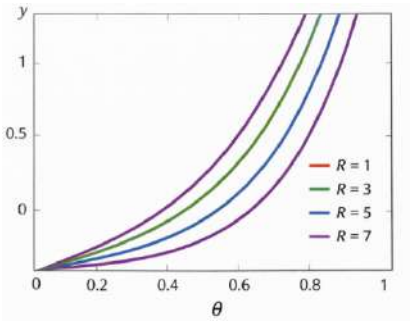

Fig 5: Effect of Radiation Parameter (R) on temperature

Radiative heat transfer increases effective thermal conductivity of the fluid enabling increased amount of heat to diffuse off the surface. This causes an increase in the thickness of the thermal boundary layer and high temperature profiles.

4.5 Effect of Heat Generation Parameter (Q)

Fig. 6 indicates the change in temperature with the parameter of heat generation Q. As can be seen temperature increases with Q.

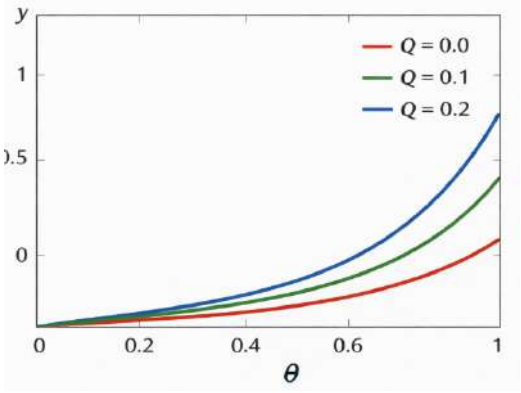

Fig. 6: Heat generation parameter (Q) on temperature

The internal heat generation provides more power to the fluid that enhances thermal diffusion and greatly adds to thermal boundary layer thickness.

4.6 Effect of Chemical Reaction Parameter (Kc)

Fig.7 is a depiction of the concentration profiles of various values of chemical reaction parameter Kc. The concentration is lowered when Kc is high.

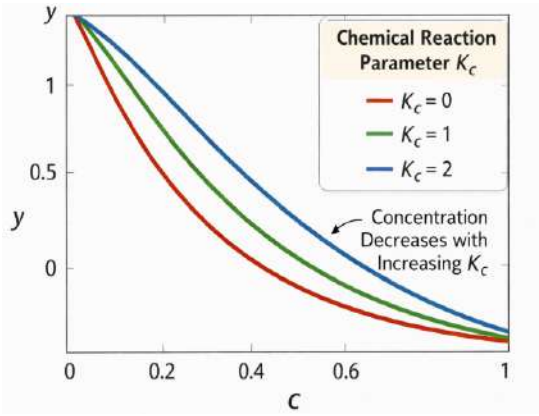

Fig. 7: Chemical reaction parameter (Kc) on concentration

This is explained by the fact that the consumption of the species is increased by the reaction of the chemicals. Increased reaction rates decrease the concentration boundary layer thickness and decrease mass diffusion.

4.7 Effect of Schmidt Number (Sc)

Fig. 8 shows the effect of Schmidt number Sc in terms of concentration distribution. It is observed that the concentration reduces as Sc increases.

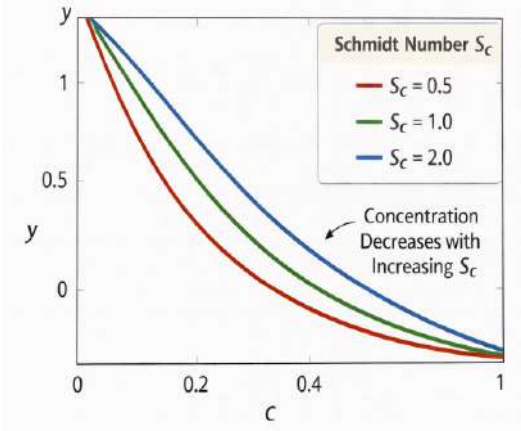

Fig. 8: Schmidt number (Sc) on concentration

The fact that Sc is the ratio of momentum diffusivity to mass diffusivity implies that the higher the Sc the lesser the mass diffusion. Consequently, the magnitude of concentration boundary layer is reduced considerably.

4.8 Discussion of Surface Transport Quantities

The variations of skin friction coefficient Cf, Nusselt number Nu, and Sherwood number Sh are computed from Eqs. (15–17).

The following trends are observed:

- Cf increases with Gr and Gc due to stronger buoyancy forces.
- Cf decreases with increasing M and β due to enhanced resistive forces.
- Nu increases with radiation parameter R and heat generation Q.
- Sh increases with Sc but decreases with increasing chemical reaction parameter Kc.

These findings are in agreement with the physical expectations and past experiments on MHD Casson fluids reported in the literature [3], [11], [12].

5. CONCLUSIONS

This paper has numerically studied the unsteady MHD Casson fluid flow past a vertical porous plate subject to the joint influence of chemical reaction, radiative heat transfer, heat generation, viscous dissipation and magnetic field using Crank Nicolson finite difference scheme. Nonlinear partial differential equations that governed it were converted into dimensionless equations and efficiently solved with the right boundary conditions. The numerical findings indicate that the Casson parameter has a profound effect on the momentum boundary layer with the magnitude of β in terms of β decreasing the velocity distribution under the effect of increasing the effective viscosity. The increase in the velocity profile of the thermal Grashof number is due to the accelerated buoyancy force whereas the magnetic parameter dampens the velocity field due to the resistive Lorentz force. Temperature distribution is dependent on radiation parameter and heat generation parameter and this implies that thermal boundary layer is thickened by diffusion of thermal energy. Conversely, the concentration profile diminishes as the chemical reaction parameter increases as the stronger the reaction rate, the lower the concentration of the species in the boundary layer. In addition, increased Schmidt numbers translate to decreased thickness of concentration boundary layer because of decreased mass diffusivity. The calculated surface values indicate that the skin friction coefficient is

a growing quantity with buoyancy parameters and a declining one with stronger magnetic and Casson effects. Nusselt number is enhanced by the effect of radiation and heat generation whereas Sherwood number is enhanced by Schmidt number and reduced by the parameter of chemical reaction. All in all, the current study gives an in-depth insight into the transport properties of Casson fluids subjected to combined effects of magnitude, radiative, and reactive magnetic, radiative, and reactive effects, which are applicable in various industrial and engineering practices.

REFERENCES

1. Crane, L. J. (1970). Flow past a stretching plate. *Zeitschrift für Angewandte Mathematik und Physik (ZAMP), 21*(4), 645–647. https://doi.org/10.1007/BF01587695
2. Pop, I., & Na, T. Y. (1996). Unsteady flow past a stretching sheet. *Mechanics Research Communications, 23*(4), 413–422. https://doi.org/10.1016/0093-6413(96)00041-7
3. Vajravelu, K. (2001). Viscous flow over a nonlinear stretching sheet. *Applied Mathematics and Computation, 124*(3), 281–288. https://doi.org/10.1016/S0096-3003(00)00062-8
4. Cortell, R. (2007). Effects of viscous dissipation and radiation on the thermal boundary layer over a nonlinearly stretching sheet. *Chemical Engineering and Processing: Process Intensification, 46*(8), 721–728. https://doi.org/10.1016/j.cep.2006.07.006
5. Chamkha, A. J. (2003). Hydromagnetic flow and heat transfer over a permeable stretching surface embedded in a porous medium. *International Journal of Engineering Science, 41*(13–14), 1427–1443. https://doi.org/10.1016/S0020-7225(03)00079-7
6. Turkyilmazoglu, M. (2011). Exact analytical solutions for heat and mass transfer of MHD slip flow in nanofluids. *International Journal of Thermal Sciences, 50*(11), 2264–2276. https://doi.org/10.1016/j.ijthermalsci.2011.06.001
7. Narayana, M., & Sibanda, P. (2012). Laminar flow of nanofluids with radiation and viscous dissipation effects. *Boundary Value Problems, 2012*, Article 146. https://doi.org/10.1186/1687-2770-2012-146
8. Raptis, A., & Perdikis, C. (1999). Radiation and free convection flow past a moving plate. *Applied Mathematics and Computation, 105*(1), 95–101. https://doi.org/10.1016/S0096-3003(98)10083-9
9. Makinde, O. D. (2005). Free convection flow with thermal radiation and mass transfer past a moving vertical porous plate. *International Communications in Heat and Mass Transfer, 32*(10), 1411–1419. https://doi.org/10.1016/j.icheatmasstransfer.2005.07.005
10. Ibrahim, S. Y., & Makinde, O. D. (2010). Radiation effect on chemically reacting MHD boundary layer flow. *Communications in Nonlinear Science and Numerical Simulation, 15*(5), 1425–1434. https://doi.org/10.1016/j.cnsns.2009.06.018
11. Pattnaik, J. R., Dash, G. C., & Singh, S. (2015). Chemical reaction effects on MHD flow over an exponentially stretching sheet. *Alexandria Engineering Journal, 54*(3), 803–812. https://doi.org/10.1016/j.aej.2015.06.006
12. Gopal, D., Kishan, N., & Reddy, J. V. R. (2016). Influence of higher-order chemical reactions on MHD nanofluid flow. *Journal of Molecular Liquids, 221*, 1089–1095. https://doi.org/10.1016/j.molliq.2016.06.070

13. Mukhopadhyay, S. (2013). Casson fluid flow and heat transfer over a stretching surface. *Journal of King Saud University – Engineering Sciences, 25*(1), 1–5. https://doi.org/10.1016/j.jksues.2011.08.004
14. Pushpalatha, K., & Reddy, N. B. (2017). Effects of thermal radiation and chemical reaction on Casson fluid flow. *Ain Shams Engineering Journal, 8*(3), 379–388. https://doi.org/10.1016/j.asej.2015.09.004
15. Abbas, Z., Sheikh, M., & Motsa, S. S. (2018). Fractional modeling of Casson fluid flow with heat and mass transfer. *Advances in Mechanical Engineering, 10*(5), 1–12. https://doi.org/10.1177/1687814018776256
16. Patel, H. R., & Singh, R. (2019). Effects of heat generation and porous medium on Casson nanofluid flow. *Results in Physics, 13*, 102245. https://doi.org/10.1016/j.rinp.2019.102245
17. Gebhart, B. (1962). Effects of viscous dissipation in natural convection. *Journal of Fluid Mechanics, 14*(2), 225–232. https://doi.org/10.1017/S0022112062001196
18. Chamkha, A. J. (1999). Effects of heat generation on convection flow. *International Journal of Heat and Fluid Flow, 20*(1), 84–89. https://doi.org/10.1016/S0142-727X(98)10042-2
19. Mitchell, A. R., & Griffiths, D. F. (1980). *The finite difference method in partial differential equations*. Wiley.
20. Morton, K. W., & Mayers, D. F. (2005). *Numerical solution of partial differential equations: An introduction* (2nd ed.). Cambridge University Press.